RSC Sustainability

ROYAL SOCIETY OF CHEMISTRY

PAPER

View Article Online
View Journal | View Issue

Cite this: *RSC Sustainability*, 2024, **2**, 1067

The use of deep eutectic solvents as a promising approach in the design of microwave-based green gas sensors†

Emilie Bertrand, *[a] Mohamed Himdi,[a] David Rondeau, [a] Xavier Castel,[a] Thomas Delhaye[a] and Ludovic Paquin [b]

Received 15th December 2023
Accepted 2nd March 2024

DOI: 10.1039/d3su00470h

rsc.li/rscsus

This study investigates a new kind of sensitive layer composed of choline chloride–urea deep eutectic solvent for microwave gas sensor application to detect HCl vapor. The sensing microwave device is based on a quarter-wavelength stub resonator operating in C-band with its gap filled with the sensitive layer. Accordingly, the microwave response of such a device depends on its exposure time to HCl vapor. Furthermore, the dielectric characteristics (ε_r and tgδ) of the sensitive layer and their variation related to HCl vapor exposure have been retrieved and checked through another microwave device specifically developed, namely a 50 Ω transmission line with a gap.

Sustainability spotlight

Today, air quality surveillance is a major societal issue for the protection of the population and a large number of detection methods are developed. Among them, there are gas sensors known for their immediate detection time and their ease-of-use. Lots of different categories of gas sensors exist such as electrochemical sensors, optical sensors, microwave sensors, *etc*. This work presents a new promising approach in the design of microwave-based green gas sensors by using deep eutectic solvents. They are a new class of green solvents known for their low toxicity, low production cost and non-volatility. Thereby, this work enables the development of a sustainable microwave gas sensor, which aligns with the 11th goal of the UN (sustainable cities and communities).

1. Introduction

The development of microwave-based gas sensors appears to be attracting increasing interest in the application field of air quality control.[1–3] Such a sensor technology is based on the modification of the dielectric characteristics of an active layer implemented in a microwave device, caused by its interactions with the surrounding volatile chemical species. The radio-frequency (RF) signal transduction is ensured by the electromagnetic response variation of the sensitive layer under microwave excitation (from 300 MHz to 300 GHz), as it interacts with the chemical gaseous compounds.[4,5]

The use of microwave gas sensors for the detection of volatile organic compounds (VOCs) or other atmospheric pollutants, such as CO_2 and NH_3, was already mentioned in the literature.[3–15] The detection measurements were associated with various microwave transduction technologies differing from their microwave topology and the sensitive material used for the gas–sensor interactions. The nature of the selected sensitive material (such as carbon nanotubes, metal-oxides, conducting polymers, polydimethylsiloxane (PDMS), *etc*.) sets the dielectric characteristic values of the active layer, namely the dielectric permittivity ε_r and the loss tangent tgδ, which will evolve during its interactions with the volatile chemical species. Thereby, the microwave response of the sensitive layer-based device will evolve too.

In the green microwave sensor development area, an active material with relevant dielectric characteristic variation capabilities and high interacting abilities with gaseous compounds is investigated here. Accordingly, deep eutectic solvents (DESs) were selected as sensitive layers.[16] The use of DESs for microwave sensor application is justified by their ionic soft material referencing,[17] used in environmentally friendly transistors[18] and involved in the development of biosensors.[19] DESs are also a new variety of green solvents first mentioned by Abbott *et al.*[20] and known for their low toxicity, non-volatility and low cost of production.[21–26] Their organization can be described through non-covalent molecular networks associating a hydrogen bond acceptor (HBA) and a hydrogen bond donor (HBD).[27–32] Examples of DES applications in chemistry were described through extraction and microextraction techniques,[33–36] electrochemistry,[37] and catalysis.[38,39] Several studies have also shown that DESs based on choline chloride were able to absorb air contaminants such as sulfur dioxide[40,41] or ammonia.[42]

[a]*Univ Rennes, CNRS, IETR – UMR 6164, F-35000 Rennes, France. E-mail: david.rondeau@univ-rennes.fr*

[b]*Univ Rennes, CNRS, ISCR – UMR 6226, F-35000 Rennes, France*

† Electronic supplementary information (ESI) available. See DOI: https://doi.org/10.1039/d3su00470h

The present paper deals with the use of a new sensitive DES-based material for the development of microwave gas sensors based on a printed quarter-wavelength stub resonator. The implementation suitability of such an active layer based on green chemistry is tested through the use of a choline chloride–urea mixture referenced as an archetypical DES. By referring to recent published studies on efficient absorption of gaseous hydrogen chloride (HCl) by deep eutectic solvents,[43] the frequency analysis and dielectric characteristic assessment of this new sensitive material can be performed with and without interaction with gaseous HCl produced close to the DES-based microwave gas sensor at room temperature. Note that for the present work, gaseous HCl is produced by a simple evaporation of aqueous HCl droplets positioned near the sensitive layer.

2. Experimental section

2.1. Chemicals

Chemicals used for the synthesis of DES are choline chloride (purity ≥ 98%) and urea (purity = 99%) purchased from Sigma-Aldrich (Saint Quentin Fallavier, France) and used without any purification. Hydrochloric acid (37% purity) was supplied by Sigma Aldrich and diluted with distilled water to reach a 1 mol L^{-1} molar concentration.

2.2. DES preparation

The DES choline chloride/urea was obtained from a mixture of choline chloride (ChCl) as the HBA and urea (U) as the HBD (Fig. 1). It was synthesized by mixing ChCl and U in a 1 : 2 molar ratio at T = 65 °C under stirring for 4 hours until a homogeneous, transparent and viscous liquid was obtained. Then, the DES was cooled down to room temperature. This led to a supramolecular network made by the association of one cholinium chloride salt and two urea molecules.[27,29–32]

2.3. Microwave device design

The microwave devices, designed for testing the performance of DES-based sensitive materials in the application field of gas sensors, were fabricated on an 18 μm-thick copper layer printed on a 0.5 mm-thick polytetrafluoroethylene (PTFE) substrate (Rogers 5880) characterized by a dielectric permittivity $\varepsilon_r = 2.1$ and a loss tangent $tg\delta = 10^{-3}$ at 10 GHz. As shown in Fig. 2, the microwave devices consisted of a 1.8 mm-wide 50 Ω transmission line with a 200 μm-wide gap located in its center. A 0.3 mm-wide quarter-wavelength stub resonator supplied by a 1.8 mm-wide 50 Ω line was also printed. A 0.08 mm-wide gap is located near the center of the stub. It provides different resonances whose frequency values depend on the material filling the gap (air or DES). It is worth noting that the bottom side not shown in Fig. 2 corresponds to a metallic ground plane. Moreover, P_1, P_2, P_1' and P_2' in Fig. 2 are the ports of the transmission line and of the quarter-wavelength stub resonator, respectively.

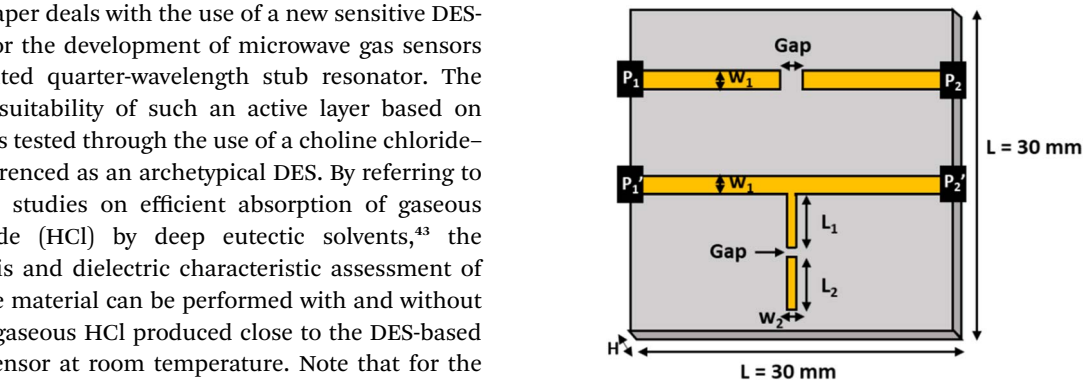

Fig. 2 Top side of the printed circuit of the microwave devices composed of a 50 Ω transmission line with a gap and a quarter-wavelength line stub associated with a gap (grey: substrate; yellow: copper layer).

Table 1 shows the dimensions of the H, w_1, w_2, gap, L_1 and L_2 parameters.

Accordingly, the present study enables (i) the validation of the proper functioning of the developed microwave devices when the DES, filling the gap, interacts with HCl vapor and (ii) the retrieval of the dielectric characteristics (ε_r and $tg\delta$) of the DES before and after its interactions with HCl vapor. A change in the resonance frequencies of the open quarter-wavelength stub resonator is expected since their values depend on the dielectric characteristic variations of the liquid filling its gap. The basic responses concern the unfilled gap (or that filled with air) and the gap filled with distilled water. As depicted in Fig. 3, the simulated S_{21} transmission coefficient responses of the quarter-wavelength stub resonator change from 9.24 GHz (unfilled gap with $\varepsilon_r = 1$ and $tg\delta = 0$ for air) to 4.32 GHz (gap filled with water with $\varepsilon_r = 85$ and $tg\delta = 0.8$ in the simulated frequency range[44]). The numerical simulations were achieved through the electromagnetic CST Microwave Studio software.[45]

2.4. Experimental setup and protocol

The effects of the gaseous HCl interactions with DES are based on a simple exposure protocol that consist in the deposition of

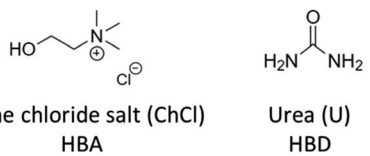

Fig. 1 Chemical structure of ChCl/U reagents.

Table 1 Dimensions of the H, w_1, w_2, gap, L_1 and L_2 parameters in Fig. 2

Parameters	50 Ω transmission line with a gap	Quarter-wavelength stub resonator with a gap
H	0.5 mm	0.5 mm
w_1	1.8 mm	1.8 mm
w_2	—	0.3 mm
Gap	0.2 mm	0.1 mm
L_1	—	5.7 mm
L_2	—	4.2 mm

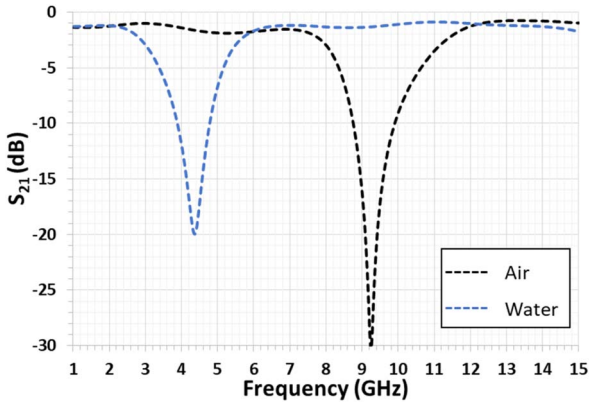

Fig. 3 Simulated transmission coefficient magnitudes of a quarter-wavelength stub resonator with an unfilled gap (air) and gap filled with water.

a 1 μL droplet of HCl aqueous solution with a concentration of 1 mol L^{-1} (10^6 μmol L^{-1}) near the DES droplet. It should be specified that the main aim of the present study is to describe a proof of concept of the use of DESs as active surfaces for microwave gas sensors. Therefore we do not focus on the relative humidity effect on the microwave device responses towards HCl interactions. Also note that the working temperature was maintained at 20 °C ± 1 °C.

The device used for validating the DES-based microwave gas sensor is shown in Fig. 4. The microwave devices were supplied by a Vector Network Analyzer (VNA) N5222A from Keysight and connected through a measurement V-Anritsu cell. Before each measurement, a short-open-load-through (SOLT) calibration step was performed to remove cabling and connector involvement of the microwave device response. After calibration, a 15 μL DES droplet was dropped onto the gap of the stub resonator. The S_{21} transmission coefficient was then recorded. Afterwards, 15 μL of HCl at 1 mol L^{-1} was placed close to the DES droplet without any contact. It is worth noting that the deposition of a single HCl droplet near the sensitive material was meant to simplify the gas sensing protocol of the study and allowed us to work safely. The gas under test was therefore a mixture of gaseous hydrogen chloride and water vapor. The effect of water vapor alone will also be assessed. Fig. 4(b) presents details of the V-Anritsu cell after the deposition of the DES droplet onto the gap of either the 50 Ω transmission line or the stub resonator, whereas the HCl droplets are spotted near these two gaps (see Fig. 2). The only possible interaction between the two liquid droplets is therefore HCl evaporation. The total exposure time was 15 min and two measurements were carried out, the first one at an intermediate time of 4 min and the second one at the final time. These exposure times were selected to get significant response variations between each measurement. The microwave measurements were carried out from 1 GHz to 15 GHz.

3. Results and discussion

3.1. Frequency analysis of ChCl/U DES dropped onto the gap of the quarter-wavelength stub resonator

Fig. 5 presents the variation of the S_{21} transmission coefficient magnitude of the quarter-wavelength stub resonator when its gap is filled with the liquid that has to be tested. With water, the measured resonance frequency shifts from 9.20 GHz to 4.28 GHz, as expected by the numerical simulation (see Fig. 3). In the diagram in Fig. 5, the minimum magnitude is −14.6 dB. This value remains higher than the simulated one of −20 dB (Fig. 3). This difference can be due to the water loss tangent value considered for the numerical simulation, which underestimates the experimental value. In the case of the so-called ChCl/U DES droplet, the resonance frequency (f_{res}) shifts from 9.20 GHz to 6.68 GHz with a S_{21} magnitude of −8.6 dB. When the DES droplet is exposed to gaseous HCl, the resonance frequency shift still increases and its magnitude decreases during the exposure time of 15 min. The reduction of the resonance magnitude associated with the enlargement of the S_{21} peak shape demonstrates an increase in the loss tangent of the sensitive material.

Regarding Fig. 6, the S_{21} magnitude difference (ΔS_{21}) *versus* frequency is computed before and after exposure to HCl for 4 min and 15 min (Fig. 6). The presence of minima and maxima is explained by the shift of the resonance's frequency, previously

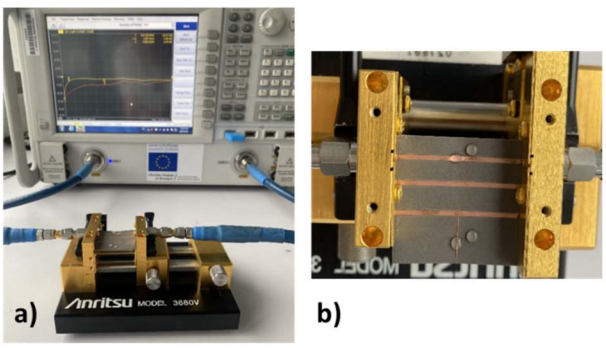

Fig. 4 (a) Experimental setup (VNA + V cell) used to validate the DES-based microwave gas sensor concept and to retrieve the dielectric characteristics (ε_r and tgδ) of the DES sensitive material; (b) details of the V-Anritsu cell after the deposition of the DES and HCl droplets.

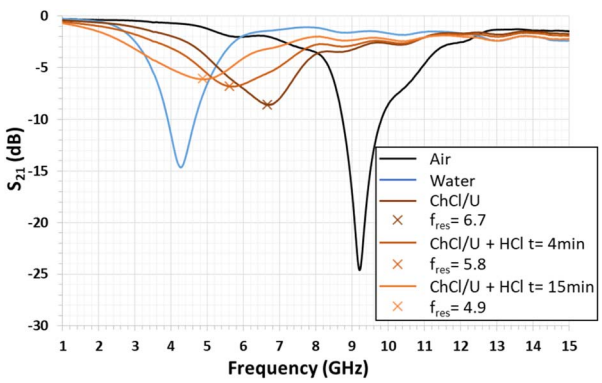

Fig. 5 Measured transmission coefficient magnitudes of the quarter-wavelength stub resonator with its gap unfilled (air), and filled with water and ChCl/U droplets (non-exposed and exposed to HCl vapor for 4 and 15 min).

highlighted in Fig. 5. For exposure times of 4 min and 15 min, the minimum levels are −2.24 dB at 4.89 GHz and −4.19 dB at 4.55 GHz, respectively. In the case of the maximum levels at the identical exposure time, these ones are 3.99 dB at 7.03 GHz and 5.46 dB at 6.98 GHz, respectively (see Fig. 6).

Note that the open literature reports the same phenomenon in the case of ammonia microwave gas sensors based on TiO_2 and SnO_2/bionic porous (BP) carbon sensitive layers. For TiO_2 layers, the magnitude response of the gas sensor was limited to 0.0007 dB.[3] For BP carbon, it was 2.5 dB.[46] In addition, for other sensitive layers based on metal–organic frameworks, a maximum sensitivity of 24 kHz per percentage of CO_2 was obtained.[47,48] In the present study, the maximum magnitude difference reaches 5.5 dB after only 15 min of exposure to gaseous HCl, demonstrating great sensibility of the DES layer to HCl.

As mentioned in the Experimental section, the studied gas is hydrated HCl in the gas phase that will be denoted as gaseous HCl further in the text. A study of the effect of H_2O vapor alone on the sensor response was also performed by dropping 15 μL of pure H_2O near the DES (in the same way as the HCl droplet). The S_{21} transmission coefficient was recorded after 4 and 15 min.

In this context, Fig. 7 presents a comparison of the magnitude differences obtained when the DES interacts with gaseous HCl and H_2O at the vapor state. By focusing on the maximum level of the curves, distilled H_2O vapor has an effect on the sensor response. Indeed, the sensor maximum level interacting with distilled H_2O vapor, after 4 min and 15 min of exposure time, is 3.32 dB at 7.06 GHz and 5.52 dB at 6.95 GHz, respectively.

This behavior was predictable through studies which highlighted that water decreases the DES viscosity. Moreover, viscosity is related to the DES conductivity.[49–51] Thus, water affects the conductivity of DES, meaning that it also modifies the transmission coefficient values. Nevertheless, the magnitude difference calculated after 4 min of HCl vapor exposure is greater than that after 4 min of distilled H_2O vapor exposure (ΔS_{21} = +0.67 dB). Thereby, the microwave sensor is sensitive to a small amount of HCl (only 1 mol L^{-1}). After 15 min of exposure, there is no difference between the S_{21} values. Presumably, water absorption by DES has a more significant impact on the resonator microwave signal and hides that of HCl.

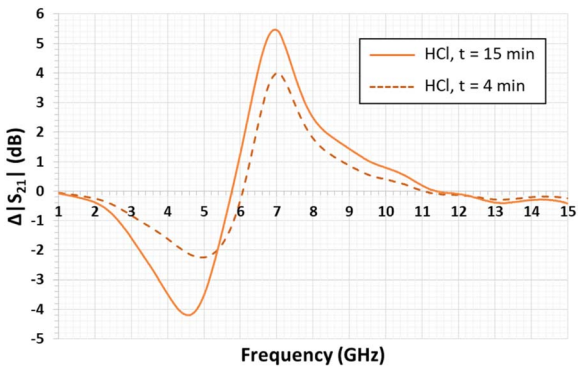

Fig. 6 Magnitude differences of transmission coefficients (ΔS_{21}) *versus* frequency values for HCl vapor exposure times of 4 min (dashed line) and 15 min (straight line). The ChCl/U DES is used as a sensitive material.

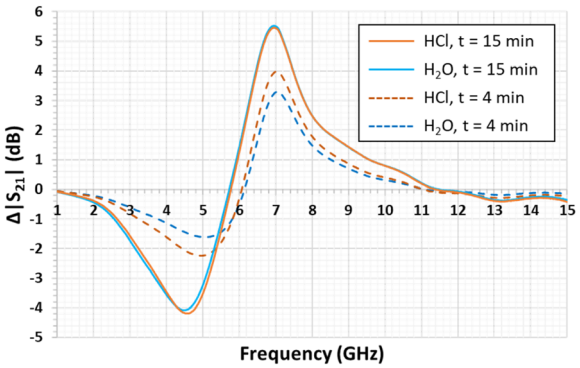

Fig. 7 Magnitude differences of transmission coefficients (ΔS_{21}) *versus* frequency values for exposure to HCl (orange lines) or water (blue lines) at two exposure times of 4 min (dashed lines) and 15 min (straight lines). The ChCl/U DES is used as a sensitive material.

This experiment demonstrates two phenomena. First, there is a sensitivity effect of the microwave sensor. Its response differs depending upon the species interacting with the DES. Second, a mixture of H_2O and HCl gives a stronger microwave response compared with that of H_2O. Therefore, this response would be even more significant with hydrogen chloride gas.

3.2. Dielectric characteristic assessment of the ChCl/U DES

The dielectric characteristics (ε_r and tgδ) of ChCl/U have been obtained by numerical simulations from the quarter-wavelength stub resonator measurements. The results of the CST simulations are illustrated in Fig. 8. The assessment was performed by matching the S_{21} numerical simulations with the measurements of resonance frequencies and magnitudes.

Table 2 shows the best agreement between simulation and measurement results. As shown in Table 2, in the case of the single DES droplet, the differences are equal to 0.1 GHz and 1.3 dB, respectively. The simulated S_{21} parameter computed from the dielectric characteristics is displayed in Fig. 9. As shown in Fig. 3 and 5, water and air are used as references.

As shown in Table 3, the dielectric permittivity of ChCl/U used as the sensitive material is $\varepsilon_r = 4.0$. This value increases under HCl exposure, reaching 6.0 at $t = 4$ min and 6.5 at $t =$ 15 min.

Despite a clear shift of the resonance peak after 15 min of HCl vapor exposure, the dielectric permittivity evolves slightly ($\varepsilon_r = 6.5$ against 4.0 for the ChCl/U DES). This is also due to the DES loss tangent value variation since, in addition to the dielectric permittivity value variation (see above), the tgδ value is 1.5, whereas the value is 0.7 prior to HCl exposure. Thus, the simulated ChCl/U dielectric values (ε_r and tgδ) and their respective variation under HCl vapor fit with the measured data. This behavior is illustrated through the comparison of Fig. 5 and 9.

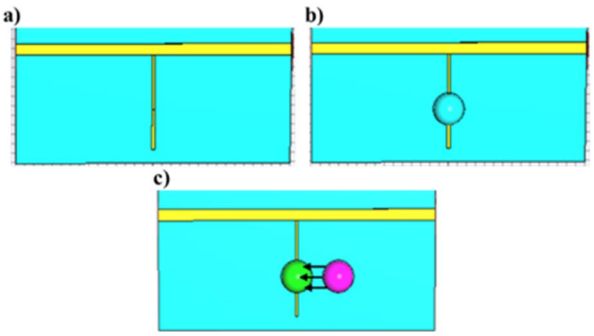

Fig. 8 Numerical simulation setup (CST software) of the ChCl/U dielectric characteristics (ε_r and tgδ) based on the quarter-wavelength stub resonator measurements with (a) an unfilled gap, (b) a gap filled with a water droplet (see the blue half-sphere) and (c) DES droplet deposition (see the green half-sphere) exposed to HCl vapor (see the pink half-sphere).

Table 2 Comparison of the theoretical and experimental S_{21} resonance frequencies and magnitudes

Exposure time to gaseous HCl	Resonance frequency (GHz)		Resonance magnitude (dB)	
	Simul.	Meas.	Simul.	Meas.
$t = 0$ min	6.60	6.68	−7.28	−8.60
$t = 4$ min	5.49	5.67	−7.54	−6.80
$t = 15$ min	4.71	4.89	−8.19	−6.10

3.3. Application to a 50 Ω transmission line with a gap

The sensing applications have been also tested on a simple microwave device, composed of a 50 Ω transmission line with a 200 μm-width gap previously shown in Fig. 2 and whose characteristics are regrouped in Table 1. The sensing behaviors have been numerically simulated through CST software, as illustrated in Fig. 10.

Two numerical simulations were performed. The first one takes solely into account the ChCl/U droplet spotted onto the transmission line gap, *i.e.* without HCl exposure for which the studied microwave device reacts like a capacitor (Fig. 11). Indeed, it appears that at low operating frequencies, the RF signal was not transmitted (S_{21} magnitude lower than −20 dB). At high frequencies, the simulation's results lead to a short-circuit behavior (S_{21} magnitude lower than −10 dB). The second numerical simulation, based on the dielectric characteristics of the DES after 15 min exposure to HCl vapor (see Table 3 for the DES dielectric characteristic values), shows an increase of the RF signal transmission at low operating frequencies (S_{21} magnitude reaches −10 dB at 1 GHz) and a better RF signal transmission at higher frequencies (S_{21} magnitude close to −7 dB at 15 GHz). This behavior is due to the increase in the ChCl/U dielectric permittivity value ($\varepsilon_r = 6.5$ against 4.0 for the raw DES).

Table 3 Values of numerical simulations of the ChCl/U dielectric characteristics (ε_r and tgδ) at different times of gaseous HCl exposure

Exposure time to gaseous HCl	Dielectric permittivity ε_r	Loss tangent tgδ
$t = 0$ min	4.0 ± 0.2	0.7 ± 0.05
$t = 4$ min	6.0 ± 0.2	0.9 ± 0.05
$t = 15$ min	6.5 ± 0.2	1.5 ± 0.05

The microwave measurements at $t = 0$ min and after 15 min gaseous HCl exposure, such as those shown in Fig. 11, disclose that the numerical simulation's results agree with the

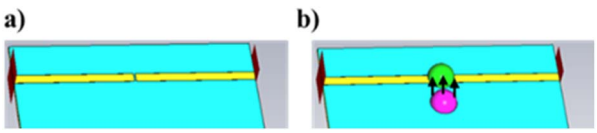

Fig. 10 Numerical simulation setup (CST software) of the 50 Ω transmission line with (a) an unfilled gap and (b) a gap filled with the ChCl/U DES droplet (see the green half-sphere) and exposed to HCl vapors (see pink half-sphere).

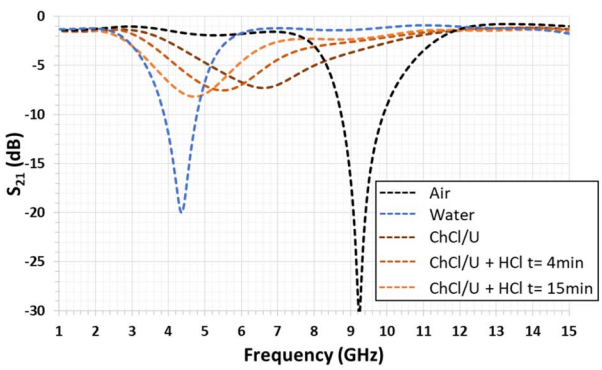

Fig. 9 Simulated transmission coefficient magnitudes of the quarter-wavelength stub resonator with its gap unfilled (air), and filled with water and ChCl/U droplets (non-exposed and exposed to HCl vapors for 4 and 15 min).

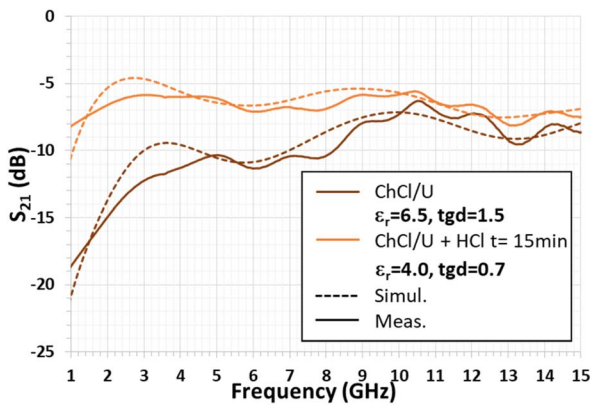

Fig. 11 Comparison of the simulated and measured transmission coefficient magnitudes of the 50 Ω transmission line with its gap filled with a ChCl/U DES droplet considered as a sensitive layer, before and after 15 min exposure to HCl vapor.

experimental data, validating the dielectric characteristic (ε_r and tgδ) values of the studied DES (see Table 3). As a result, it can be claimed that a viscous materiel based on the deposition of a ChCl/U DES droplet can be used as a sensitive layer to gaseous HCl exposure.

4. Conclusion

The present paper highlights that a quarter-wavelength stub resonator with its gap filled by a DES can be used to get relevant dielectric characteristics (ε_r and tgδ) of deep eutectic solvent exposed to gaseous HCl. This DES is composed of a mixture of choline chloride and urea, and can be considered as a sustainable sensitive material in the application field of green microwave gas sensors. The fair values are indeed 4.0 and 0.7 for ε_r and tgδ, respectively, in the case of the non-exposed DES, whereas they increase up to 6.5 and 1.5, respectively, after 15 min of exposure to gaseous HCl. This has been also disclosed through complementary microwave measurements based on a simple device made of a 50 Ω transmission line with a gap. In this case too, the ChCl/U material exhibits high sensitivity to gaseous HCl. With the aim of active layer elaboration for microwave gas sensor application, further studies should be performed to assess not only the reversibility of the interaction between gaseous HCl and such DES-based microwave gas sensors, but also their responses towards HCl exposure, considering then the influence of the working temperature and the composition of the exposure medium. The applications to sensitivity assessments of other hazardous air contaminants, such as sulfur dioxide or ammonia, are in progress. Moreover, the implementation of such a sensitive material into microwave systems based on printed antennas would be also useful for the development of wireless gas sensor systems. Note that the use of sensitive layers based on DESs for microwave and antenna gas sensor application has been recently patented by some of us.[52]

Conflicts of interest

There are no conflicts to declare.

Acknowledgements

This work was supported in part by the European Union through the European Regional Development Fund, in part by the Ministry of Higher Education and Research, in part by the Région Bretagne, and in part by the Département des Côtes d'Armor and Saint-Brieuc Armor Agglomération through the CPER Projects 2015–2020 MATECOM and SOPHIE/STIC&Ondes.

Notes and references

1 P. Grundler, *ChemTexts*, 2017, **4**, 3–16.
2 B. de Fonseca, J. Rossignol, D. Stuerga and P. Pribetich, *Urban Clim.*, 2015, **14**, 502–515.
3 G. Bailly, A. Harrabi, J. Rossignol, D. Stuerga and P. Pribetich, *Sens. Actuators, B*, 2016, **236**, 554–564.
4 J. Jouhannaud, J. Rossignol and D. Stuerga, *C. R. Phys.*, 2007, **8**, 456–461.
5 G. Barochi, J. Rossignol and M. Bouvet, *Sens. Actuators, B*, 2011, **157**, 374–379.
6 M. Dragoman, A. Muller, D. Neculoiu, G. Konstantinidis, K. Grenier, D. Dubuc, L. Bary, R. Plana, H. Hartnagel, E. Fourn and E. Flahaut, in *Proc. Eur. Microw. Conf.*, Munich, Germany, 2007, pp. 16–19.
7 H. Lee, G. Shaker, K. Naishadham, X. Song, M. McKinley, B. Wagner and M. Tentzeris, *IEEE Trans. Microwave Theory Tech.*, 2011, **59**, 2665–2673.
8 J. Rossignol, G. Barochi, B. de Fonseca, J. Brunet, M. Bouvet, A. Pauly and L. Markey, *Sens. Actuators, B*, 2013, **189**, 213–216.
9 D. Aloisio and N. Donato, *Procedia Eng.*, 2014, **87**, 1083–1086.
10 B. H. Kim, Y. J. Lee, H. J. Lee, Y. Hong and J. G. Yook, in *Proc. IEEE Sens.*, Valencia, Spain, 2014, pp. 1815–1818.
11 Y.-J. Lee, B.-H. Kim, H.-J. Lee, Y. Hong and J.-G. Yook, in *Proc. IEEE Sens.*, Valencia, Spain, 2014, pp. 1819–1822.
12 C. Pardue, K. Naishadham, X. Song and M. Swaminathan, in *Proc. Wirel. Microw. Technol. Conf.*, WAMICON, Tampa, FL, USA, 2014, pp. 1–3.
13 W. T. Chen, K. M. E. Stewart, R. R. Mansour and A. Penlidis, *Sens. Actuators, A*, 2015, **230**, 63–73.
14 B. de Fonseca, J. Rossignol, I. Bezverkhyy, J. P. Bellat, D. Stuerga and P. Pribetich, *Sens. Actuators, B*, 2015, **213**, 558–565.
15 M. H. Zarifi, A. Sohrabi, P. M. Shaibani, M. Daneshmand and T. Thundat, *IEEE Sens. J.*, 2015, **15**, 248–254.
16 V. Agieienko and R. Buchner, *Phys. Chem. Chem. Phys.*, 2020, **22**, 20466–20476.
17 L. C. Tomé and D. Mecerreyes, *J. Phys. Chem. B*, 2020, **124**, 8465–8478.
18 F. Pettersson, T. Remonen, D. Adekanye, Y. Zhang, C.-E. Wilén and R. Österbacka, *ChemPhysChem*, 2015, **16**, 1286–1294.
19 R. Svigelj, N. Dossi, C. Grazioli and R. Toniolo, *Sensors*, 2021, **21**, 4263–4281.
20 A. P. Abbott, G. Capper, D. L. Davies, R. K. Rasheed and V. Tambyrajah, *Chem. Commun.*, 2003, **1**, 70–71.
21 Y. Dai, J. van Spronsen, G.-J. Witkamp, R. Verpoorte and Y. H. Choi, *Anal. Chim. Acta*, 2013, **766**, 61–68.
22 C. Florindo, F. Lima, B. Dias Ribeiro and I. M. Marrucho, *Curr. Opin. Green Sustainable Chem.*, 2019, **18**, 31–36.
23 Q. Zhang, K. De Oliveira Vigier, S. Royer and F. Jérôme, *Chem. Soc. Rev.*, 2012, **41**, 7108–7146.
24 A. Paiva, R. Craveiro, I. Aroso, M. Martins, R. L. Reis and A. R. C. Duarte, *ACS Sustain. Chem. Eng.*, 2014, **2**, 1063–1071.
25 E. L. Smith, A. P. Abbott and K. S. Ryder, *Chem. Rev.*, 2014, **114**, 11060–11082.
26 B. B. Hansen, S. Spittle, B. Chen, D. Poe, Y. Zhang, J. M. Klein, A. Horton, L. Adhikari, T. Zelovich, B. W. Doherty, B. Gurkan, E. J. Maginn, A. Ragauskas, M. Dadmun, T. A. Zawodzinski, G. A. Baker, M. E. Tuckerman, R. F. Savibell and J. R. Sangoro, *Chem. Rev.*, 2021, **121**, 1232–1285.

27 H. Sun, Y. Li, X. Wu and G. Li, *J. Mol. Model.*, 2013, **19**, 2433–2441.
28 S. L. Perkins, P. Painter and C. M. Colina, *J. Chem. Eng. Data*, 2014, **59**, 3652–3662.
29 C. R. Ashworth, R. P. Matthews, T. Welton and P. A. Hunt, *Phys. Chem. Chem. Phys.*, 2016, **18**, 18145–18160.
30 O. S. Hammond, D. T. Bowron and K. J. Edler, *Green Chem.*, 2016, **18**, 2736–2744.
31 C. F. Araujo, J. A. P. Coutinho, M. M. Nolasco, S. F. Parker, P. J. A. Ribeiro-Claro, S. Rudic, B. I. G. Soares and P. D. Vaz, *Phys. Chem. Chem. Phys.*, 2017, **19**, 17998–18009.
32 L. Percevault, T. Delhaye, A. Chaumont, R. Schurhammer, L. Paquin and D. Rondeau, *J. Mass Spectrom.*, 2021, **56**, e4725.
33 B. Tang, H. Zhang and K. H. Row, *J. Sep. Sci.*, 2015, **38**, 1053–1064.
34 S. C. Cunha and J. O. Fernandes, *Trends Anal. Chem.*, 2018, **105**, 225–239.
35 M. B. Arain, E. Yilmaz and M. Soylak, *J. Mol. Liq.*, 2016, **224**, 538–543.
36 M. Soylak and M. Koksal, *Microchem. J.*, 2019, **147**, 832–837.
37 A. P. Abbott, *Green Sustainable Chem.*, 2022, **36**, 100649.
38 B. Singh and H. Lobo, *Catal. Lett.*, 2011, **141**, 178–182.
39 P. Liu, J.-W. Hao, L.-P. Mo and Z.-H. Zhang, *RSC Adv.*, 2015, **5**, 48675–48704.
40 D. Yang, M. Hou, H. Ning, J. Zhang, J. Ma, G. Yang and B. Han, *Green Chem.*, 2013, **15**, 2261–2265.
41 S. Sun, Y. Niu, Q. Xu, Z. Sun and X. Wei, *Ind. Eng. Chem. Res.*, 2015, **54**, 8019–8024.
42 F. Zhong, H. Peng, D.-J. Tao, P.-K. Wu, J.-P. Fan and K. Huang, *ACS Sustain. Chem. Eng.*, 2019, **7**, 3258–3266.
43 L. Feng, H. Meng, Y. Lu and C. Li, *Sep. Purif. Technol.*, 2022, **281**, 1–11.
44 U. Kaatze and V. Uhlendorf, *Z. Phys. Chem.*, 1981, **126**, 151–165.
45 CST, *Computer Simulation Technology*, **https://www.cst.com**.
46 N. Wang, N. Zhang, T. Wang, F. Liu, X. Wang, X. Yan, C. Wang, X. Liu, P. Sun and G. Lu, *Sens. Actuators, B*, 2022, **350**, 130854.
47 M. H. Zarifi, A. Gholidoust, M. Abdolrazzaghi, P. Shariaty, Z. Hashisho and M. Daneshmand, *Sens. Actuators, B*, 2018, **255**, 1561–1568.
48 M. Fayaz, M. J. Lashaki, M. Abdolrazzaghi, M. H. Zarifi, Z. Hashisho, M. Daneshmand, J. E. Anderson and M. Nichols, *Sens. Actuators, B*, 2019, **282**, 218–224.
49 Q. Zhang, K. De Oliveira Vigier, S. Royer and F. Jérôme, *Chem. Soc. Rev.*, 2012, **41**, 7108–7146.
50 C. Du, B. Zhao, X. B. Chen, N. Birbilis and H. Yang, *Sci. Rep.*, 2016, **6**, 29225.
51 D. Lapeña, L. Lomba, M. Artal, C. Lafuente and B. Giner, *J. Chem. Thermodyn.*, 2019, **128**, 164–172.
52 D. Rondeau, E. Bertrand, X. Castel and M. Himdi, French Patent, FR23/07528, 2023.